Chapter 11
Firing Rate Models

One of the most common ways to model large networks of neurons is to use a simplification called a firing rate model. Rather than track the spiking of every neuron, instead one tracks the averaged behavior of the spike rates of groups of neurons within the circuit. These models are also called population models since they can represent whole populations of neurons rather than single cells. In this book, we will call them rate models although their physical meaning may not be the actual firing rate of a neuron. In general, there will be some invertible relationship between the firing rate of the neuron and the variable at hand. We derive the individual model equation in several different ways, some of the derivations are rigorous and are directly related to some biophysical model and other derivations are ad hoc. After deriving the rate models, we apply them to a number of interesting phenomena, including working memory, hallucinations, binocular rivalry, optical illusions, and traveling waves. We also describe a number of theorems about asymptotic states as well as some of the now classical work on attractor networks.

There are many reasons to use firing rate models. First of all, there is the obvious issue of computational efficiency. Modeling a network of thousands of individual conductance-based neurons can tax even the fastest computers. For this reason, many large-scale simulations use simple spiking models such as the integrate-and-fire model. In many experimental preparations, what is measured is not the intracellular potential of neurons, but instead the probability of firing. This type of recording is done with an extracellular electrode and thus spikes can be detected but the other aspects of the cell are unknown. Hence, to better make better comparisons with experiments, it makes sense to consider the firing rate instead of the potential. Field potential recordings, electroencephalograms, and functional magnetic resonance imaging presumably represent large populations of neurons. Thus, a model at this scale may be better posed in terms of population equations.

Rate models are among the oldest forms of modeling of the brain and the nervous system, going back to the late 1930s. Cowan and Sharp [50] have written a very comprehensive history of the early days of neural network research. A nice oral history of the subject of neural nets can be found in [5].

Rate models are essentially the underlying "biology" in the very popular and useful theory of neural networks. For example, the "connectionist" models developed under the Parallel Distributed Processing program by McClelland and Rumelhart

G.B. Ermentrout and D.H. Terman, *Mathematical Foundations of Neuroscience*, Interdisciplinary Applied Mathematics 35, DOI 10.1007/978-0-387-87708-2_11,

[196] and the "back propagation" models are all connected to the wet nervous system (albeit, occasionally rather tenuously) via rate models. Massively recurrent attractor networks, perceptrons, hidden layer models, adaptive resonance theory (and its descendants) are all essentially rate models [98]. We will spend little time in this chapter on the more machinelike and abstract ideas of neural network theory and will instead focus on the connection of rate models to biophysics and the usefulness of these networks in modeling biological phenomena.

11.1 A Number of Derivations

11.1.1 Heuristic Derivation

We start with a very simple, somewhat abstract derivation that was advocated in early work of Cowan and later formalized in Ermentrout and Cowan [69]. Figure 11.1 shows a schematic for a pair of neurons with a synapse from one to the other. The measurable output is the firing rate, $u_i(t)$, which depends in a nonlinear way on the somatic potential, $V_i(t)$:

$$u_i(t) = F_i(V_i(t)).$$

Now, the reader might recall that most of our biophysical models produced firing rates as a function of the applied current, so she may be puzzled at the use of voltage as a driver for the output of the cell. We justify this by assuming the current flowing into the axon hillock (which is the site of action potentials) is proportional to the voltage drop between the soma and the resting potential of the hillock compartment. Thus, the somatic potential is passively converted to an axon hillock current via Ohm's law, that is, $I = V/R_{\mathrm{M}}$, where R_{M} is the membrane resistance. Each time a presynaptic cell fires a spike, a postsynaptic potential appears at the soma. The size of this potential, as well as the sign, depends on the nature of the synapse, the position on the dendrite, and so on. We define $\Phi_{ij}(t)$ to be the postsynaptic

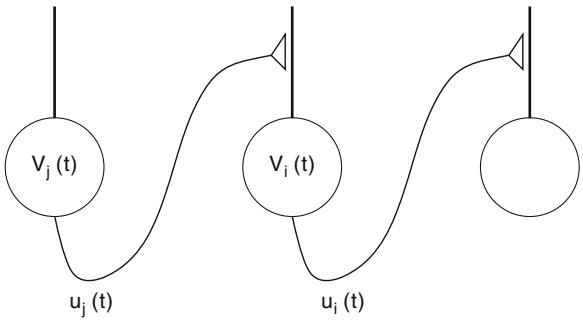

Fig. 11.1 Schematic of a pair of neurons synaptically coupled

potential appearing on postsynaptic cell i due to a single spike from presynaptic cell j. Let $t_1, t_2, \ldots, t_m$ be the firing times of the presynaptic cell. By assuming linear summation of the postsynaptic potentials, the total potential received at the soma is

$$G_{ij}(t) = \sum_l \Phi_{ij}(t - t_l).$$

The firing rate $u_j(t)$ determines the instantaneous number of spikes that a neuron fires in an infinitesimal time interval. That is, we can think of $u_j(t)\mathrm{d}t$ as the probability of a spike occurring in the time interval $(t, t + \mathrm{d}t)$. Thus, the above sum can be rewritten as

$$G_{ij}(t) = \int_{t_0}^{t} \Phi_{ij}(t - s)u_j(s - \tau_{ij})\mathrm{d}s,$$

where τ_{ij} is the possible axonal delay in the spike arising at cell j arriving at cell i. If the effects of each cell linearly sum, then we can close this model, resulting in an integral equation for either V_i or u_i:

$$V_i(t) = \sum_j G_{ij}(t) = \sum_j \int_{t_0}^{t} \Phi_{ij}(t - s)F_j(V_j(s - \tau_{ij}))\mathrm{d}s, \tag{11.1}$$

$$u_i(t) = F_i\left(\sum_j \int_{t_0}^{t} \Phi_{ij}(t - s)u_j(s - \tau_{ij})\mathrm{d}s\right). \tag{11.2}$$

Both of these rather formidable equations can be greatly simplified once we have discussed the postsynaptic potential function $\Phi_{ij}(t)$. To do this, let us consider a passive membrane with a time constant τ_m and into which a presynaptic current is injected:

$$\tau_m \frac{\mathrm{d}\Phi}{\mathrm{d}t} + \Phi = R_{\mathrm{M}} I(t).$$

For simplicity, suppose $I(t)$ is an alpha function of the form

$$I(t) = \exp(-t/\tau_d) - \exp(-t/\tau_r).$$

Here, τ_d is the decay of the synaptic current and τ_r is the rise time of the current. Assuming $\Phi(0) = 0$, we can solve this simple differential equation to obtain the postsynaptic voltage response:

$$\Phi(t) = \frac{\tau_d}{\tau_d - \tau_m}\left(\mathrm{e}^{-t/\tau_d} - \mathrm{e}^{-t/\tau_m}\right) - \frac{\tau_r}{\tau_r - \tau_m}\left(\mathrm{e}^{-t/\tau_r} - \mathrm{e}^{-t/\tau_m}\right). \tag{11.3}$$

This response depends on three parameters: the postsynaptic time constant and the presynaptic rise and decay times. One could make this response function far more complex by including dendritic filtering properties and so on as long as it remains linear. (If the response is nonlinear, then we cannot simply sum the inputs from different neurons, nor can we even sum the individual postsynaptic potentials to form the integral.)

The Volterra integral equations (11.1) and (11.2) are not simple to analyze so one generally attempts to convert them into differential or differential-delay equations. For $\Phi(t)$ represented as a finite sum of exponentials, we can always invert the integral equation to form a set of differential equations. To see this, consider first the simple integral equation

$$x(t) = \int_{t_0}^{t} \mathrm{e}^{-(t-s)/\tau} y(s-r)\mathrm{d}s,$$

where r is the possible delay. Differentiate x with respect to t to obtain

$$\frac{\mathrm{d}x}{\mathrm{d}t} = y(t-r) - \frac{1}{\tau}\int_{t_0}^{t} \mathrm{e}^{-(t-s)/\tau} y(s-r)\mathrm{d}s = y(t-r) - x(t)/\tau.$$

Thus, we see that $x(t)$ satisfies

$$\frac{\mathrm{d}x}{\mathrm{d}t} + x/\tau = y(t-r).$$

If $\Phi(t)$ is the sum of several exponentials, then we can break the Volterra integral equation into a set of differential equations using the above identity.

This approach is not entirely satisfactory since for each connection $\Phi_{ij}(t)$ we need (in the present case) three differential equations. If the network of interest consists of a homogeneous population of neurons, that is, their synaptic time constants are the same and they have the same membrane time constant, then we can write $\Phi_{ij}(t) = w_{ij}\Phi(t)$, where w_{ij} represent the magnitudes of the connections. Suppose the delays, τ_{ij} are the same for all cells, say, $\tau_{ij} = r$. Then the voltage equation (11.1) now becomes

$$(LV_i)(t) = \sum_j w_{ij} F_j(V_j(t-r)), \tag{11.4}$$

where L is a linear homogeneous differential operator. Equation (11.4) is essentially the classical model for a neural network. We can similarly reduce (11.2) to a set of differential equations. Let

$$z_i(t) = \int_{t_0}^{t} \Phi(t-s)u_i(s-r)\mathrm{d}s.$$

Thus,

$$(Lz_i)(t) = u_i(t-r) = F_i\left(\sum_j w_{ij} z_j(t-r)\right). \tag{11.5}$$

This is not quite the same as an equation for the firing rate, $u_i(t)$, but this variable is obtained easily from $z_i(t)$ by differentiation [217]. $z_i(t)$ is the *synaptic drive*.

This drastically simplifies the simulation and analysis of single populations of differential equations but we are still stuck with difficulties when we have, say, an excitatory and an inhibitory population. Key to the reduction was the idea that $\Phi_{ij}(t) = w_{ij}\Phi(t)$. However, if we examine (11.1) carefully, we see that we can make a less restrictive assumption that $\Phi_{ij}(t) = w_{ij}\Phi_i(t)$ for then we obtain

$$(L_i V_i)(t) = \sum_j w_{ij} F_j(V_j(t-r)).$$

Similarly, examining (11.2), if we assume $\Phi_{ij}(t) = w_{ij}\Phi_j(t)$, then we obtain

$$(L_i z_i)(t) = F_i\left(\sum_j w_{ij} z_j(t-r)\right).$$

Rather than a system of N^2 differential equations for a network of N neurons, we just have N differential equations. Thus, we now want to examine more closely what these two assumptions entail.

Suppose $\Phi_{ij} = w_{ij}\Phi_i(t)$. This means the response of neuron i to any inputs depends (up to a scalar constant which could be negative or positive) only on the properties of the *postsynaptic* cell. This assumption is valid if the shape and temporal properties of the presynaptic currents are the same no matter what type the presynaptic cell is. This kind of model would fail to distinguish between, say, a slow NMDA current and a fast AMPA current, or even between the fast AMPA and somewhat slower GABA currents. However, looking at (11.3), we see that if $\tau_m \gg \{\tau_d, \tau_r\}$, then $\Phi(t) \approx \exp(-t/\tau_m)/\tau_m$, which is independent of the presynaptic timescales. That being the case, our system of differential equations is first order:

$$\tau_{m,i}\frac{\mathrm{d}V_i(t)}{\mathrm{d}t} + V_i(t) = \sum_j w_{ij} F_j(V_j(t-r)). \tag{11.6}$$

Equation (11.6) is commonly used as a model neural network and within the scope of our derivation, the timescale associated with each element in the network is that of the *membrane time constant.*

Now, suppose $\Phi_{ij} = w_{ij}\Phi_j(t)$. This means the shape of the postsynaptic potential depends only on the *presynaptic* cell. To us, this is a more reasonable assumption since we can distinguish different types of synapses (and, below, this allows us to incorporate synaptic depression and potentiation). Suppose the rise time of the synapse and the membrane time constant of the postsynaptic cell are small compared with the decay of the synapse. Then $\Phi_j(t) \approx \exp(-t/\tau_d)/\tau_d$ and, as above, we derive the following equation for the *synaptic drive*:

$$\tau_d\frac{\mathrm{d}z_i(t)}{\mathrm{d}t} + z_i(t) = F_i\left(\sum_j w_{ij} z_j(t-r)\right). \tag{11.7}$$

This model is also a very popular version for neural networks. In this case, the temporal dynamics are dominated by the synaptic decay, τ_d.

Equations (11.6) and (11.7) are often regarded as equivalent, but in the present derivation, they are not. Rather, they represent two distinct assumptions about the dominant timescales.

Before discussing the forms of the firing rate functions, F_i, we turn to a derivation based on the theory of averaging and some assumptions about the types of bifurcation in the conductance-based models.

11.1.2 Derivation from Averaging

Consider the following conductance-based network:

$$C\frac{\mathrm{d}V_i}{\mathrm{d}t} + I_i(V_i,\ldots) = -\sum_j g_{ij}s_j(V_i - V_{\mathrm{syn},j}), \tag{11.8}$$

$$\tau_{\mathrm{syn}}\frac{\mathrm{d}s_i}{\mathrm{d}t} + s_i = R_i(V_i, s_i). \tag{11.9}$$

Here, I_i represents all the nonlinear conductances which lead to action potentials. To simplify the derivation, we have assumed a synapse from cell j produces the same conductance change regardless of the postsynaptic target. This is not an unreasonable assumption. Weakening this assumption results in more differential equations just as the more general assumptions in the previous section. Suppose $\tau_{\mathrm{syn}} \gg 1$. This means the synapses are slow. If the synapses are slow, then $s_i(t)$ will change very slowly relative to the dynamics of the membrane; thus, we can treat s_i as constant. For ease in exposition, we will suppose all the neurons are excitatory, which means $V_{\mathrm{syn},j} = V_e$. Let $G_i = \sum_j g_{ij}s_j$. Since s_j are roughly constant, so is G_i, so we can treat it as a parameter. Equation (11.8) is now isolated from the rest of the population because G_i is just a constant. We can compute the bifurcation diagram of the membrane potential and obtain

$$V_i(t) = \bar{V}_i(t; G_i).$$

We will assume only two types of behavior: stable fixed points or limit cycles. In the latter case, we assume the period is $T_i(G_i)$. We now return to the synaptic equations (11.9) but substitute $\bar{V}_i(t; G_i)$ for V_i since the potential changes on a faster timescale than the synapses. Thus, (11.9) becomes

$$\frac{\mathrm{d}s_i}{\mathrm{d}t} = \frac{1}{\tau_{\mathrm{syn}}}(-s_i + R_i(\bar{V}_i(t; G_i), s_i)).$$

If $\bar{V}_i$ is a stable fixed point, then the s_i equation is straightforward since the right-hand side is independent of t. However, if $\bar{V}_i$ is periodic, then we are still safe since we can apply the averaging theorem and obtain

$$\frac{\mathrm{d}s_i}{\mathrm{d}t} = \frac{1}{\tau_{\mathrm{syn}}}(-s_i + \langle R_i(\bar{V}_i(t;G_i), s_i)\rangle),$$

where

$$\langle R_i(\bar{V}_i(t;G_i), s_i)\rangle = \frac{1}{T_i(G_i)}\int_0^{T_i(G_i)} R_i(\bar{V}_i(t;G_i), s_i)\mathrm{d}t \equiv Q_i(G_i, s_i).$$

Thus, since all the quantities involved depend on G_i, we have reduced this conductance-based model to a system of first-order equations for the synaptic gates, s_i:

$$\tau_{\mathrm{syn}}\frac{\mathrm{d}s_i}{\mathrm{d}t} + s_i = Q_i\left(\sum_j g_{ij}s_j, s_i\right). \tag{11.10}$$

We now explore (11.10), specifically $Q(G,s)$, in more detail. In Chap. 8, we modeled synapses as

$$\frac{\mathrm{d}s}{\mathrm{d}t} = \alpha(V)(1-s) - \beta s$$

in much the same way as we model channels. Factoring out the $\beta = 1/\tau_{\mathrm{syn}}$, we see that $R(V,s) = \alpha(V)\tau_{\mathrm{syn}}(1-s)$. The function $\alpha(V)$ is zero except when the neuron spikes. Let us suppose the width of a spike is independent of the firing rate of the neuron, so

$$\int_0^T \alpha(\bar{V}(t))\tau_{\mathrm{syn}}\mathrm{d}t = \mu,$$

where μ is a constant essentially independent of T, the period. Let us define

$$F(G) \equiv \frac{1}{T(G)}$$

as the firing rate of the conductance-based model given synaptic conductance G. Then, with these approximations

$$Q_i(G_i, s_i) \equiv \frac{1}{T_i(G_i)}\int_0^{T_i(G_i)} R_i(\bar{V}_i(t;G_i), s_i)\mathrm{d}t = \mu_i F_i(G_i)(1-s_i).$$

Putting all these terms together, we can now write (11.10) as

$$\tau_i\frac{\mathrm{d}s_i}{\mathrm{d}t} = \mu_i F_i\left(\sum_j g_{ij}s_j\right)(1-s_i) - s_i. \tag{11.11}$$

With the exception of the $(1-s)$ term, (11.11) is the same as (11.7). This makes sense, for in both cases the timescale is the synaptic decay. Here, the variable $s_i(t)$

is the fraction of open synaptic channels, whereas in (11.7), $z_i(t)$ was called the synaptic drive.

If there are different types of synapses, say, excitatory and inhibitory, the synaptic current is

$$I_{\text{syn}} = G_{\text{ex}}(V - V_{\text{ex}}) + G_{\text{in}}(V - V_{\text{in}})$$

and the period, T, is a function of two variables, G_{ex} and G_{in}. This may seem to be a problem since it is not clear how T should depend on the two conductances; we would like it to be additive or some simple functional. If the conductance-based neuron is operating near a saddle–node bifurcation, then we know that

$$F(I_{\text{syn}}) \approx K\sqrt{I_{\text{syn}} - I^*},$$

where I^* is the critical current at which the saddle–node appears. Let V^* be the potential at the saddle–node. Then (at least near the saddle–node)

$$I_{\text{syn}} = G_{\text{ex}}(V^* - V_{\text{ex}}) + G_{\text{in}}(V^* - V_{\text{in}}),$$

so the firing rate is an *additive* function of the inhibitory and excitatory conductances.

The big advantage of deriving firing rate models from conductance-based models using averaging is that it is simple to incorporate slow currents such as spike-frequency adaptation and also short-term synaptic plasticity. We will introduce some of these models later and others will be provided as exercises.

11.1.3 Populations of Neurons

The derivations above were motivated by considering a single conductance-based neuron and then from this deriving a model for the firing rate. However, the main role of firing rate models is not to mimic single cells, but rather to examine large numbers of neurons in some "average" fashion. We can draw the analogy between intracellular and extracellular recordings in physiology. Intracellular recording enables one to track the membrane potential of a single neuron. Extracellular recordings, such as the local field potential, represent the responses of many neurons. Sharp electrodes (also extracellular) can resolve spikes of individual neurons. However, these spiking events are probabilistic, so experimentalists repeat the same stimulus over many trials to obtain a poststimulus time histogram. The poststimulus time histogram has units in spikes per unit time (often milliseconds), so it is effectively a rate. The intuition behind the poststimulus time histogram is that it is *assumed to be true* that if we were able to record simultaneously from 100 nearby locations, we would get the same result as from recording from one location 100 times. For this to be reasonable, we have to assume the neurons fire largely independently of each other. Once this assumption has been made, then we see that the firing rate of

the population is exactly the same as that of an individual neuron and the equations derived in the previous section can thus be interpreted as the population firing rate. However, in the derivation from averaging, the firing rate function is deterministic. Thus, if every cell were identical, then all cells would fire in perfect concert. Thus, we need to account for differences between neurons when we treat populations. One way to do this is to include the effects of noise. In Chap. 10, we saw that extrinsic noise can smooth the firing rate as a function of the input current. Thus, for example, we could replace a firing rate function $F = \sqrt{I}$ by a smoothed version of this which has a nonzero firing rate even for subthreshold inputs ($I < 0$). Another way to smooth the firing rate function is to assume heterogeneity. For example, suppose the firing rate is $F(I - I^*)$ for $I > I^*$ and zero otherwise as would be the case for a saddle–node on an invariant circle bifurcation. If the threshold values I^* are taken from some distribution, $Q(I)$, then we can write an "average" firing rate function

$$F_Q(I) = \int Q(I^*)F(I - I^*)\mathrm{d}I^*. \tag{11.12}$$

We will leave it as an exercise for the reader to explore specific forms for the averaged firing rate.

Let us give a quick derivation of a typical firing rate or population model. Consider N identical neurons which receive (possibly random inputs) and between which there are recurrent connections. We will assume, for simplicity, all the neurons are excitatory (multiple types of neurons are easily generalizable) and the connections are all identical as are the inputs, the strengths of which are scaled by $1/N$. Each neuron undergoes dynamics

$$C\frac{\mathrm{d}V_i}{\mathrm{d}t} = -I_{\mathrm{ion},i} + \bar{g}s_i(V_i - E_{\mathrm{syn}}),$$

where $\bar{g}s_i$ is the conductance felt by each neuron. Since all inputs are excitatory and we assume the recurrent synapses have dynamics similar to the dynamics of the input synapses, we have

$$(Ls_i)(t) = J_T\sum_k \delta\left(t - t_k^T\right) + \sum_{j,k} J_{ij}\delta\left(t - t_k^j\right),$$

where L is a linear differential operator which governs the synapse. Alternatively, we could generalize this and write

$$s_i(t) = \int_{t_0}^{t} \alpha(t - t')\left(J_T\sum_k \delta\left(t' - t_k^T\right) + \sum_{j,k} J_{ij}\delta\left(t' - t_k^j\right)\right)\mathrm{d}t'. \tag{11.13}$$

Here, t_k^T are the spike times from the inputs and t_k^j are the spike times of the jth cell in the network.

Key to the notion of population models is the fact that we assume the neurons are firing independently of each other within the network. Is this a good assumption? If there is a great deal of extrinsic independent noise, then it is likely that there are few correlations between neighboring neurons. A given population of interest often receives inputs from an earlier processing stage. (For example, layer 4 in the cortex receives inputs from the thalamus.) If the incoming action potentials come from randomly chosen subsets of the input layer, then we expect that spiking within the output layer would be uncorrelated. However, it turns out that this seemingly obvious assumption is not true. In recent experiments, Reyes [224] examined the following scenario. From N independent Poisson trains of spikes, a subset of $m \ll N$ was selected and injected into a neuron. The spike times of this neuron were recorded. A different set of m spikes was selected and the experiment was repeated until there were N new spike trains. These formed the basis for a repeat of the first set of experiments; N new spike trains were collected from these spike trains and so on. By layer 10 (ten iterations), there was considerable synchrony between the spike trains, so it was no longer reasonable to assume independence. The reason for this is that even though each trial shared only a few inputs, these inputs were enough to become amplified over multiple layers, leading to synchrony. Thus, the assumption of independence is at best an approximation and at worst is wrong. In the Reyes experiment, there was no recurrent coupling between cells within a layer. Recurrent connections can either increase or decrease the synchrony, depending on the nature of the coupling. Indeed, we saw in Chap. 8 that synaptic timescales, intrinsic currents, and the sign of the coupling can all have dramatic effects on the synchronization between coupled neurons. Since the only theory that has been done on the issue of asynchrony is for very simple models (leaky integrate and fire, quadratic integrate and fire), little more can be said about the assumption of independence for recurrently connected neurons.

There is one last issue that we want to discuss before moving on to applications of firing rate models. This is the issue of time constants. Figure 11.1 showed that a noisy integrate-and-fire model with high noise could follow a stimulus rather robustly if we added a small time constant to the dynamics. Specifically, let $I(t)$ be a time-varying input and let $F(I)$ be the noisy firing rate as a function of the constant input [cf. (11.19) or (11.20)]. Then the firing rate for a time-varying stimulus is

$$\tau_f \frac{\mathrm{d}f}{\mathrm{d}t} = -f + F(I(t)).$$

The parameter τ_f is ad hoc and chosen to be small. It is not related to a membrane or synaptic time constants but depends on all of these as well as the characteristics of the noise [90]. With low noise, then the instantaneous firing rate can be very complicated. In Project 2, we suggest a way to look at these dynamics.

11.2 Population Density Methods

Gerstner and Kistler [99] provided a quick derivation for firing rate models of whole populations of neurons. Cai et al. [32] also derived such models. The equations which result are similar to those that we derived for globally coupled oscillators in Chap. 9. Basically, in all the derivations, the authors start with simple models for neurons such as the leaky integrate-and-fire model and from these derive an equation for the distribution of the potential. The flux of the potential across threshold is the firing rate of the cells. In general, the equations which result from these derivations are difficult to solve and often require special numerical methods. That said, they are still much faster to solve than the full network of spiking neurons. We will eschew a detailed study of the differences between the various derivations and sketch a fairly general equation based on the work of Gerstner and Kistler, which to us is the most transparent derivation. Thus, this section is closely related to Sect. 6.2 in [99]. We will approach it slightly more generally so that the resulting model is not tied to the specific form of the leaky integrate-and-fire neuron. The idea is to consider a one-dimensional neural model with some reset conditions.

We will write

$$\frac{\mathrm{d}v_i}{\mathrm{d}t} = f(v_i) + g(v_i)I_i(t),$$

where f is the spiking dynamics, g is the response to inputs, and I_i is all the synaptic currents coming into the cell. If the model requires reset, then we have the condition that when $v_i = \theta$, v_i is reset to $v_\mathrm{r} < \theta$. For example, the leaky integrate-and-fire model has $f(v) = -v/\tau$ and $g(v) = R/\tau$, where R is the membrane resistance. We define

$$\int_u^{u+\Delta u} p(u,t)\mathrm{d}u = \lim_{N\to\infty}\left(\frac{\text{no. of cells with } u < v_i(t) \le u + \Delta u}{N}\right).$$

The function $p(u,t)$ is the membrane potential density. We have the following normalization:

$$\int_{-\infty}^{\theta} p(u,t)\mathrm{d}u = 1.$$

This says that the probability is conserved. The firing rate or population activity, $A(t)$, is defined as the flux of cells across the threshold:

$$A(t) = J(\theta, t).$$

We will define this flux shortly. Neurons which cross the threshold reappear at the reset value, v_r, so this must be added to the evolution equations in the form of a source term $A(t)\delta(v - v_\mathrm{r})$. We remark that these discontinuities will disappear if we use a model such as the theta model instead of the leaky integrate-and-fire model since the "threshold" at π is just part of the full cycle. We assume all neurons receive the same external input, $I_\mathrm{ext}(t)$, and that there is random background input.

Excitatory and inhibitory synaptic inputs are allowed as well. Synapses of type k occur at rate $\nu_k(t)$. These could be from external sources or from within the network if it is recurrent. To avoid adding an additional equation, we will assume the synaptic inputs are in the form of delta functions. Consider the single cell

$$\frac{\mathrm{d}v}{\mathrm{d}t} = f(v) + g(v)w\delta(t - t^*),$$

where t^* is the time of the input and w is the amplitude. If v is the value right before t^*, then $v + wg(v) \equiv G(v, w)$ is the value of the potential right after the input. For the derivation we provide below to be valid, we will assume the function $G(v, w)$ is invertible with respect to v. In Exercise 5, you are invited to show that for small w the inverse of G is

$$H(v, w) \equiv G^{-1}(v, w) = v - g(v)w + g'(v)g(v)w^2 + O(w^3). \tag{11.14}$$

We note that if $g(v)$ is constant, then the inverse is exact. For the theta model, $g(v) = 1 + \cos v$, where $v = \pi$ is the spike. Cai et al. [32] considered $g(v) = (v_\mathrm{s} - v)$, where v_s is the synaptic reversal potential. An exact inverse can be found in this case.

With these asides out of the way, we continue the derivation. Each synapse of type k has an amplitude of w_k and occurs at rate $\nu_k(t)$. The dynamics satisfy

$$\begin{aligned}\frac{\partial p(v,t)}{\partial t} = &-\frac{\partial}{\partial v}\left((f(v) + g(v)I_\mathrm{ext}(t))p(v,t)\right) \\ &+ \sum_k \nu_k(t)[p(H(v,w_k),t)H_v(v,w_k) - p(v,t)] + A(t)\delta(v - v_\mathrm{r}).\end{aligned} \tag{11.15}$$

The first term on the right-hand side is just the drift due to the uncoupled dynamics of each neuron. The last term is the reinjection of cells which cross through the threshold for spiking. The middle term is the gain of cells which were at $H(v, w_k)$ and jumped to v owing to the synaptic input as well as the loss of those which jump from v to $G(v, w_k)$. The strange term H_v multiplying the probability arises because we want to conserve total probability. Note that it is bounded because G is invertible and thus monotonic. We remark that $p(v, t) = 0$ for $v > \theta$. Right away, we can see that there is trouble lurking about if you are interested in simulation. Equation (11.15) is a functional partial differential equation because of the term H appearing *as an argument* of the density p. The firing rate is determined from the flux across the threshold. To determine this, we rewrite (11.15) as a continuity equation. Note that

$$\nu_k[p(H(v,w_k),t)H_v(v,w_k) - p(v,t)] = -\frac{\partial}{\partial v}\nu_k \int_{H(v,w_k)}^{v} p(u,t)\mathrm{d}u.$$

Thus, for any v, (11.15) can be written as

$$\frac{\partial p}{\partial t} = -\frac{\partial J}{\partial v} + A(t)\delta(v - v_\mathrm{r}),$$

where

$$J(v,t) = [f(v) + g(v)I_{\text{ext}}(t)]p(v,t) + \sum_k \int_{H(v,w_k)}^{v} p(u,t)\,\mathrm{d}u.$$

Note that $J(v,t) = 0$ for $v > \theta$. If w_k is small, then we can expand this equation in a Taylor series to obtain the diffusion approximation. From (11.14),

$$\int_{H(v,w_k)}^{v} p(u,t)\mathrm{d}u \approx \int_{v-w_k g(v)+w_k^2 g'(v)g(v)}^{v} p(u,t)\mathrm{d}u.$$

Applying the fundamental theorem of calculus, this integral is approximately

$$w_k g(v)p(v,t) - \frac{1}{2}\left[w_k^2 g(v)^2 p(v,t)\right]_v.$$

With this approximation, the diffusive approximation for the population density equation is

$$\frac{\partial p(v,t)}{\partial t} = A(t)\delta(v - v_{\text{r}}) - \frac{\partial J_D(v,t)}{\partial v}, \tag{11.16}$$

where

$$J_D(v,t) = \left[f(v) + g(v)(I_{\text{ext}}(t) + \sum_k w_k \nu_k(t))\right] p(v,t) \tag{11.17}$$
$$-\frac{1}{2}\frac{\partial}{\partial v}\left(\sum_k \nu_k(t) w_k^2 g(v)^2 p(v,t)\right).$$

Since these are just partial differential equations, they are amenable to numerical solution. If the inputs $\nu_k(t)$ are external, then we can define

$$\sigma^2(t) = \sum_k \nu_k(t) w_k^2$$

and

$$r(t) = I_{\text{ext}}(t) + \sum_k \nu_k(t) w_k.$$

If everything is stationary, then

$$J_D(v,t) = [f(v) + g(v)r]p(v,t) - \frac{\sigma^2}{2}\frac{\partial g^2(v)p(v,t)}{\partial v},$$

where r and σ^2 are constant. Solving the steady-state equations is identical to solving the single noisy integrate-and-fire model we studied in Chap. 10.

If we are using a discontinuous neural model, such as the leaky integrate-and-fire model, then we have $p(\theta, t) = 0$ and the firing rate, $A(t)$, is given by

$$A(t) = J_D(\theta, t) = -\frac{1}{2}\frac{\partial}{\partial v}\left(\sum_k v_k(t) w_k^2 g(v)^2 p(v,t)\right)\Bigg|_{v=\theta}.$$

However, if we instead use a continuous model on the circle such as the theta model, then the equations are considerably simpler. The term $A(t)\delta(v - v_r)$ no longer appears since the natural flow of the dynamics takes v through π and the domain of the model is $[0, 2\pi)$. In this case, we get

$$A(t) = J_D(\pi, t) = f(\pi) p(\pi, t)$$

since, for the theta model, $g(\pi) = 0$. For time-dependent inputs to the theta model (or other ring models), we can solve the full equations by writing $p(x, t)$ in a finite Fourier series and then writing differential equations for the coefficients. See Project 5 in Chap. 8.

Because the partial differential equations that result from these models can be quite difficult to solve (when the noise is low), we will generally use simple ordinary differential equation forms of population models.

11.3 The Wilson–Cowan Equations

One of the most influential models in the neural network literature is the one developed by Hugh Wilson and Jack Cowan in the early 1970s [287]. The original equations have the following form:

$$\begin{aligned} \tau_e \frac{\mathrm{d}E}{\mathrm{d}t} &= -E + (1 - r_e E) F_e(\alpha_{ee} E - \alpha_{ie} I + T_e(t)), \\ \tau_i \frac{\mathrm{d}I}{\mathrm{d}t} &= -I + (1 - r_i I) F_i(\alpha_{ei} E - \alpha_{ii} I + T_i(t)), \end{aligned} \tag{11.18}$$

where T_j is the input from the thalamus and r_e and r_i represent the refractory fraction of the neurons available to fire. The term $(1 - r_e E)$ is an approximation of

$$1 - \int_{t-r_e}^{t} E(s)\mathrm{d}s,$$

which represents the fraction of neurons available to fire given they have an absolute refractory period of r_e. Curtu and Ermentrout [52] analyzed the behavior of the original integrodifferential equations for a single excitatory population. The extra premultiplicative factor $(1 - r_e E)$ does not make too much of a difference in the

analysis of the equations, so we will generally set $r_e = r_i = 0$. We first consider a single scalar model for one recurrent population of neurons. Then we turn to the pair and we will look at mutually excitatory, inhibitory, and mixed populations. The last case is the Wilson–Cowan equations.

A Note on the Gain Functions: What should one use for a gain function, $F(u)$? The traditional form for this is the logistic function, $F(u) = 1/(1 + \exp(-\beta(u - u_T)))$, which we have also encountered in our study of voltage-gated conductances. With the use of a logistic function, we interpret the function F as a probability of firing rather that an actual firing rate. A similar choice for F is $F(u) = 1 + \text{erf}(u)$, where $\text{erf}(u)$ is the error function (integral of a Gaussian). Pinto et al. [219] used this model to study the mean-field approximation for a model of cortex.

If we regard F as an actual firing rate of a single cell, then we could use an approximation for a neuron which undergoes a saddle–node bifurcation of periodic firing; namely,

$$F(u) = A\sqrt{\max(u - u_T)},$$

where u_T is the minimal current needed to induce firing. This gain function is continuous, but not differentiable and so will lead to problems when it comes time to numerically analyze models. In the presence of noise, we saw in Chap. 10 that the function is smoothed out. The following two variants of the above function are good approximations to the noisy firing rate:

$$F(u) = A\sqrt{(u - u_T)/(1 - \exp(-(u - u_T)/\beta))}, \tag{11.19}$$

$$F(u) = A\sqrt{\beta \log[1 + \exp((u - u_T)/\beta)]}. \tag{11.20}$$

Here, β is a measure of the "noise"; as $\beta \to 0$, both of these functions approach a pure square-root model. There are two more functions which are commonly encountered:

1. The step function, for which the neuron either is not firing at all or is firing at the maximal rate. This turns out to be the easiest to analyze and we will return to it when we get to networks.
2. The piecewise linear function

$$F(u) = \max(u - u_T, 0).$$

Linearity makes it possible to also analyze this function.

For the most part, there is little to recommend for the piecewise linear function other than it can be analyzed. The main objection we have for this function is that the firing rate can become infinite in recurrent networks. The step function and the logistic function, which both saturate, do not suffer from this problem. The square-root model is sublinear for large inputs, so it, too, does not "run away."

11.3.1 Scalar Recurrent Model

As a warmup problem, we consider the simple recurrent neural network model:

$$\frac{\mathrm{d}u}{\mathrm{d}t} = -u + F(\alpha u + \beta),$$

where β is the input and α is the strength of the connections. We leave as an exercise the analysis of this scalar model. We will assume $F(u) \geq 0$, $F'(u) > 0$, so the firing rate is a monotonic function. If the connections are inhibitory, $\alpha < 0$, then there is a unique asymptotically stable equilibrium point. If the connections are excitatory, then the situation is more interesting. In many firing rate functions, the derivative $F'(u)$ has a single maximum (that is, F has a single inflection point). If this is the case, then you should be able to show that there are at most three fixed points of the scalar neural network. In general, if the nonlinear gain function $F(u)$ has $2m + 1$ inflection points and aside from these $F''(u)$ is nonzero, then it is possible for the recurrent excitatory neural network to have $2m + 3$ fixed points of which $m + 1$ are stable.

To analyze bifurcations in a scalar firing rate model, we consider the current to be a parameter and ask when there is a saddle–node bifurcation. The condition is straightforward:

$$-1 + \alpha F'(\alpha u + \beta) = 0. \tag{11.21}$$

Since $F'(u)$ has a single maximum, if α is sufficiently large, then we can choose u so that (11.21) has two roots. Given such a u, say, $\bar{u}$, we plug this into the equilibrium condition and solve for β:

$$\bar{u} = F(\alpha \bar{u} + \beta).$$

Since F is invertible, we can solve for β. If α is chosen to be precisely the reciprocal of the maximum of F', then the two saddle–node roots of (11.21) merge at a codimension-2 cusp point. For more complex functions F with multiple inflection points, it is possible to have even higher codimension bifurcations such as the "butterfly catastrophe" [49].

11.3.2 Two-Population Networks

Beer [11] provided a fairly exhaustive study of two-population networks. Here, we concentrate on a few interesting cases.

We dispense with networks for which the interactions between the cells are the same, excitatory or inhibitory. The following theorem allows us to concentrate on fixed points alone:

Theorem. *Consider the planar system*

$$x' = f(x, y),$$
$$y' = g(x, y),$$

such that $f_y g_x > 0$ *for all* (x, y). *Then there are no limit cycles.*

With some hints, we leave the proof of this to the reader. We note that this bears a resemblance to Bendixon's negative criterion, which states that if $f_x + g_y$ is of fixed sign in a region, R, then there will be no limit cycles contained wholly in R.

An obvious consequence of this is that for the two-population neural model

$$\begin{aligned} \tau_1 u_1' &= -u_1 + F_1(w_{11}u_1 + w_{12}u_2), \\ \tau_2 u_2' &= -u_2 + F_2(w_{21}u_1 + w_{22}u_2). \end{aligned} \tag{11.22}$$

If $F_j'(u) > 0$ and $w_{12}w_{21} > 0$, then there are no limit cycles and there are just fixed points; thus, the entire phase portrait can be worked out by looking at the intersections of the nullclines. We will suppose F_j are saturating nonlinearities with a maximum of 1 and a minimum of 0 without loss of generality. We also assume they are monotonic and have a single inflection point. Let G_j be the inverse of F_j. Let $G_j(x)$ have vertical asymptotes at $x = 0$ and $x = 1$ and be monotonically increasing. The u_1 nullcline has the form

$$u_2 = (G_1(u_1) - w_{11}u_1)/w_{12} \equiv H_1(u_1).$$

If $w_{11} < 0$, then H_1 is a monotonic function much like G_1. However, if $w_{11} > 0$, then if the self-connection is large enough, the function H_1 has a cubic shape. Similar considerations hold for the u_2-nullcline: if $w_{22} > 0$, it can have a "cubic" shape. Figure 11.2a and b shows several different possibilities. We can freely shift the u_1-nullcline up and down by varying the inputs and the u_2-nullcline left and right as well. Up to nine fixed points are possible or as few as one. Bifurcations are generically saddle–nodes (although below we consider an important symmetric situation which results in a pitchfork). Consider the case when both nullclines are "cubic." Thus, we can define the outer and middle branches of the cubic. Any fixed point which occurs on the intersection of two outer branches is a stable node. Any fixed point occurring on two inner branches is an unstable node. The rest are saddle points. We leave this as an exercise for the interested reader. Saddle points are important

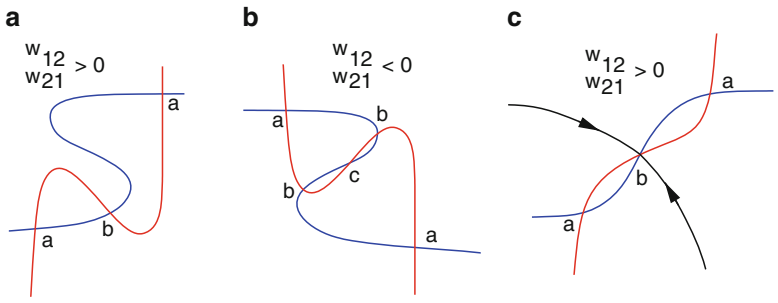

Fig. 11.2 Nullcline configurations for mutually excitatory–inhibitory networks: (**a**) mutual excitation, (**b**) mutual inhibition, (**c**) mutual excitation with weak self-connections

since their stable manifolds form separatrices dividing the plane into the domains of attraction for multiple stable fixed points. Figure 11.2c shows such an example. There are two states of this mutually excitatory network, one where both populations are firing at a low rate and one where both populations are firing at a high rate.

Before turning to the excitatory–inhibitory networks which show the richest dynamics, we consider an important example that will appear throughout this chapter and plays a fundamental role in later sections. Many cognitive and other processes require making a choice between two or more competing sensory inputs. Suppose you have a trusty musket and on your left is a charging lion and on your right a charging pug. To which do you attend? There, the choice is rather obvious. However, suppose instead of the lion, you are confronted by another pug. Then, most likely, unless you like dogs or are afraid of them, you will ignore them. Instead, if you are being charged by two lions, it is likely you will select one of them at random (if one is a bit closer, then there will be a strong bias) and stick with it.

Figure 11.3a shows a model for competition between two neural pools, labeled 1 and 2. Each receives an input and inhibits the other pool. Since this example illustrates many of the mathematical concepts we will encounter later, we will sketch

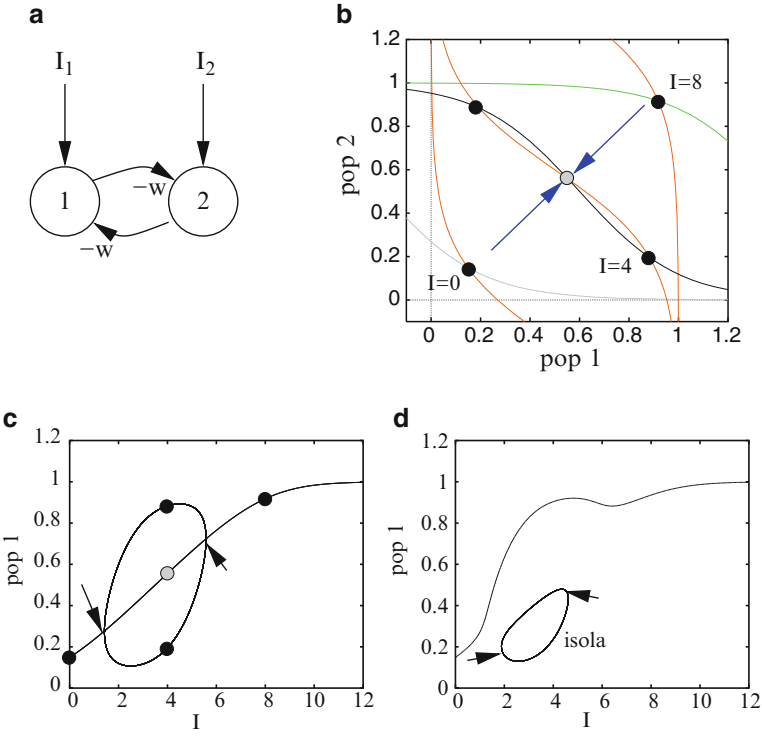

Fig. 11.3 The simplest model for competition between two populations: (**a**) the circuit, (**b**) nullclines for identical inputs at three different strengths, (**c**) bifurcation diagram when the inputs are identical, and (**d**) same as (**c**) but there is a small bias in favor of population 1

most of the details. We write $I_1 = I(1 + a)$ and $I_2 = I(1 - a)$, where a is an asymmetry parameter and I is the total input. When $a = 0$, the input is unbiased and does not favor either unit (think of the two charging pugs). The extreme asymmetry case (lion vs. pug) would have $a = \pm 1$. We will restrict our analysis to $a = 0$ and leave the $a \neq 0$ case for numerical analysis. The equations for this case are

$$\begin{aligned} u_1' &= -u_1 + F(I - wu_2), \\ u_2' &= -u_2 + F(I - wu_1). \end{aligned} \tag{11.23}$$

We will assume F is a monotonically increasing positive function with $F'(x) \to 0$ as $x \to \infty$ and we assume F is bounded as well. The weight $w \geq 0$. *Because of the symmetry*, one solution to this equation is homogeneous, $u_1 = u_2 = \bar{u}$ and

$$\bar{u} = F(I - w\bar{u}).$$

We leave as an exercise the proof that there is a unique homogeneous equilibrium point, that it is positive, and that it is a monotonically increasing function of I and monotonically decreasing function of w. Let $c = F'(I - w\bar{u}) > 0$ be the derivative of F at the equilibrium value. The linearization of (11.23) is

$$\begin{aligned} v_1' &= -v_1 - cwv_2, \\ v_2' &= -v_2 - cwv_1. \end{aligned}$$

This is a simple 2×2 matrix, A, but rather than immediately writing down the eigenvalues, we step aside for a moment to discuss matrices of a special form, so-called circulant matrices.

ASIDE.

Let $a_0, \ldots, a_{n-1}$ be fixed numbers (real or complex) and consider the matrix A formed as follows:

$$A = \begin{pmatrix} a_0 & a_1 & \ldots & a_{n-1} \\ a_{n-1} & a_0 & \ldots & a_{n-2} \\ \vdots & \vdots & \ddots & \vdots \\ a_1 & a_1 & \ldots & a_0 \end{pmatrix}.$$

Such a matrix is called a *circulant* matrix and the eigenvectors and eigenvalues are easy to write down. Let $z_k = \exp(2\pi \mathrm{i} k/n)$ for $k = 0, \ldots, n-1$. Let $\mathbf{v}_k$ be the column vector whose jth entry is z_k^{j-1}. Then $\mathbf{v}_k$ is an eigenvector for A and the eigenvalue is

$$\lambda_k = \sum_{j=0}^{n-1} a_j z_k^j.$$

For example, if $n = 2$, then the eigenvectors are $(1, 1)^{\mathrm{T}}$ and $(1, -1)^{\mathrm{T}}$, with eigenvalues $a_0 + a_1$ and $a_0 - a_1$, respectively.

END ASIDE

Since the linearization A is a circulant matrix, the eigenvectors and eigenvalues are $\{(1,1), -1-cw\}$ and $\{(1,-1), -1+cw\}$. The first of these eigenvalues is always negative; thus, any *homogeneous* perturbation (along the eigenvector, $(1,1)$) decays to zero. However, if w is large enough, then $-1+cw$ can become positive for a range of inputs I, which means asymmetric perturbations [along the eigenvector $(1,-1)$] will grow in time. At a critical value of the input, say, I_0, the asymmetric eigenvalue will be zero and we expect a bifurcation to occur. Since this problem has symmetry, the bifurcation at a zero eigenvalue will not be the generic fold, but rather a pitchfork bifurcation. This is typical in systems in which a circulant matrix is involved (that is, there is a symmetry.) Since the growth will be along the asymmetric eigenvector, the bifurcation solutions will have the form

$$(u_1, u_2) = (\bar{u} + r, \bar{u} - r),$$

where $|r|$ is the amplitude of the solution. r can be either positive or negative, corresponding to u_1 "winning" or u_2 "winning." Figure 11.3b shows the phase plane and nullclines for (11.23), where $F(u) = 1/(1 + \exp(-(u-1)))$, $w = 5$, and I is a parameter. At low inputs, both units fire equally at the same value. For intermediate values of the inputs, the homogeneous fixed point is unstable and there are two stable fixed points corresponding to one of the two units "winning." The saddle point (gray circle) has a stable manifold (blue arrows) which separates the phase plane into two regions; those in the upper-left region tend to the u_2-dominant fixed point and those in the lower-right region tend to the u_1-dominant fixed point. Thus, without any input bias, the final outcome of the competition depends on any initial activity of the two units. At high inputs, once again, the homogeneous solution is the only solution and both units fire at high rates. Figure 11.3c shows the bifurcation diagram for the symmetric input case. For I between the two arrows, one or the other population of neurons is dominant. If there is a slight bias in the inputs, then as the input increases, the favored population will always win (Fig. 11.3d), but with a strong enough perturbation it is possible to switch to the less favored population for a limited range of inputs. This figure shows what is called an *isola*, a small island of solutions. The arrows denote a pair of fold bifurcations. As the bias disappears, the isola grows and merges with the main branch of solutions to give the diagram shown in Fig. 11.3c. As the bias a increases, the isola shrinks to a point and disappears.

This example illustrates the basic concept underlying *symmetry-breaking* instabilities and bifurcations and pattern formation. The symmetric solution loses stability owing to the negative interactions and results in new solutions which are no longer so symmetric.

11.3.3 Excitatory–Inhibitory Pairs

We turn our attention to two population models in which one population is excitatory and the other inhibitory:

$$\tau_1 u_1' = -u_1 + F(w_{11}u_1 - w_{12}u_2 + I_1), \tag{11.24}$$

$$\tau_2 u_2' = -u_2 + F(w_{21}u_1 - w_{22}u_2 + I_2). \tag{11.25}$$

u_1 (u_2) is the excitatory (inhibitory) population. It is possible to do a fairly comprehensive local bifurcation analysis of this system if the inputs are the main parameters. Borisyuk and Kirillov [18] provided such an analysis when $F(u) = 1/(1 + \exp(-u))$; Hoppensteadt and Izhikevich [128] performed a similar analysis. Choosing this F has the advantage of allowing us to note that

$$\frac{\mathrm{d}F}{\mathrm{d}u} = F(1 - F).$$

Let

$$G(y) = \ln \frac{y}{1 - y}$$

be the inverse of $F(u)$. At an equilibrium point, we can solve for I_j:

$$I_j = G(u_j) - w_{j1}u_1 + w_{j2}u_2. \tag{11.26}$$

Let $B_j = w_{j1}u_1 - w_{j2}u_2 + I_j$ be the total input into each population. The linearization matrix has the form

$$A = \begin{pmatrix} -1 + w_{11}F'(B_1) & -w_{21}F'(B_1) \\ w_{12}F'(B_2)/\tau & (-1 - w_{22}F'(B_2))/\tau \end{pmatrix}.$$

We can rewrite $F'(B_j) = u_j(1 - u_j)$ using the fact that at equilibrium, $F(B_j) = u_j$ and that $F' = F(1 - F)$. There are two types of bifurcations of interest for this model: Hopf and saddle–node bifurcations. Saddle–nodes can be visualized by examining intersections of the nullclines. For the Wilson–Cowan network, there can be up to five different fixed points. Hopf bifurcations can be easily found using the identities above. Recall that a necessary condition for there to be imaginary eigenvalues for A is that the trace of A vanishes:

$$\mathrm{Tr} \equiv -1 + w_{11}u_1(1 - u_1) - 1/\tau - w_{22}u_2(1 - u_2)/\tau = 0.$$

Clearly, since $0 < u_j < 1$, the trace is always negative unless $w_{11} > 4$, so there must be sufficient recurrent excitation. We solve the above equation for $u_1 = U_1^{\pm}(u_2)$; there are two roots since it is quadratic. Plugging u_1 as a function of u_2 into (11.26), we can parameterize I_1 and I_2 by the single number u_2. Letting u_2 range between 0 and 1 for each of the two branches, $U_1^{\pm}(u_2)$, we get curves of Hopf points. This same method is not useful for the curve of folds (where the determinant vanishes) since the determinant is a quartic function of u_1 and u_2 and so not readily solvable.

The easiest way to compute bifurcation diagrams is through numerical methods. Figure 11.4 shows the behavior of this network for a fixed set of weights and time constants. As the excitatory input increases, the resting state increases until it loses stability at a Hopf bifurcation. Since increasing I_1 lifts the u_1-nullcline up, we can

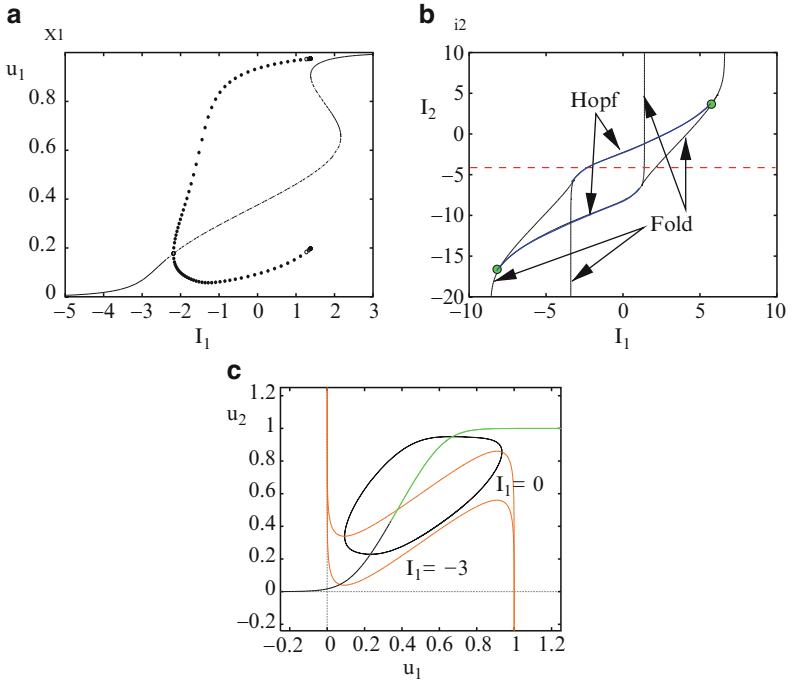

Fig. 11.4 Sample bifurcation diagram for an excitatory and inhibitory population. The parameters are $w_{11} = 12$, $w_{12} = 10$, $w_{21} = 16$, $w_{22} = 4$, and $\tau = 2$. (**a**) Behavior of u_1 as I_1 increases, $I_2 = -4$. (**b**) Two-parameter diagram as a function of the inputs, I_1, I_2. *Green circles* indicate Takens–Bogdanov points. (**c**) Phase plane for $I_2 = -4$, $I_1 = 0$

see the effect by looking at Fig. 11.4c. At negative inputs, the excitatory nullcline intersects at a point where the slope of the nullcline is negative and thus the fixed point is stable. As input increases, the intersection moves to the middle branch and for sufficient input becomes unstable. This leads to a Hopf bifurcation and limit cycle. Note that as the input increases, the excitatory nullcline gets closer and closer to the upper part of the inhibitory nullcline, so the period of the limit cycle increases. For sufficient input, there is an intersection of the nullclines at high values of excitation and inhibition.

11.3.3.1 Up–Down States

Experiments [247] in prefrontal cortical slices show that local recurrent networks of excitatory and inhibitory neurons are able to produce epochs of sustained firing both spontaneously and through stimulation. These two states (firing and quiescent) are observed in extracellular and intracellular recordings of neurons. Figure 11.5a shows an example of a recording from a cortical slice preparation with inhibition and

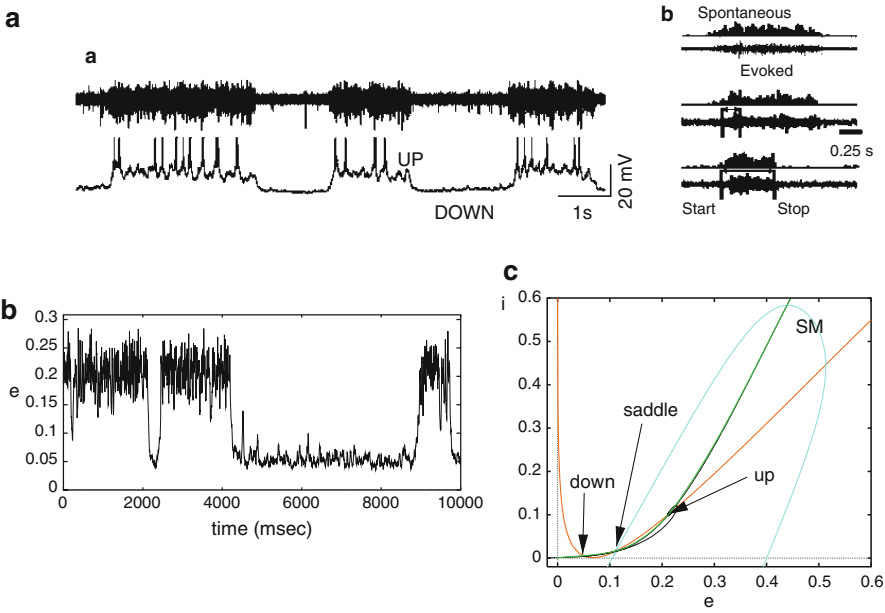

Fig. 11.5 Modeling up and down states in cortex. (**a**) Experimental data from Shu et al. [247] showing (*a*) extracellular (*upper curve*) and intracellular (*lower curve*) recordings over about 10 s, and (*b*) evoked states via external stimuli. (**b**) Simulation of up–down states in a noisy Wilson–Cowan model showing spontaneous switching. (**c**) Phase-plane explanation of the balanced bistable state. The parameters are $\tau_1 = 5$, $\tau_2 = 3$, $w_{11} = 16$, $w_{21} = 24$, $w_{12} = 10$, $w_{22} = 6$, $I_1 = -3.7$, and $I_2 = -6.7$. Colored noise is added to the inputs. *SM* stable manifold

excitation intact. The network undergoes bouts of sustained activity lasting up to 4 s followed by quiescence. Intracellular recordings of a pyramidal cell in the network show that during the bouts of activity, the membrane potential is depolarized ("up state") compared with that during the quiescent period ("down state"). Stimuli allow one to switch from the down to the up state and vice versa. Importantly, depolarizing stimuli can switch the network from the up to the down state. Furthermore, when the network is in the down state, very strong stimuli cause a brief bout of activity immediately followed by a return to the down state. These two properties allow us to make some good guesses as to what the local dynamics must be. Figure 11.5b shows a simulation of (11.24) and (11.25) when there is colored noise added to the inputs. The noise is needed to effect spontaneous switching between states. Holcman and Tsodyks [125] proposed a model for this phenomenon using recurrent excitation and synaptic depression and no inhibition. Here, we suggest a very simple explanation for the properties of up and down states using a combination of excitation and inhibition. Figure 11.5c shows the phase plane in the absence of noise for the simulation shown in Fig. 11.5b. As one would expect, there are two stable fixed points corresponding to the up and down states in the network. Separating these states is a saddle point whose stable manifold acts as a threshold. In bistable systems such as

that shown in Fig. 11.3b, the stable manifold is such that only negative perturbations of state (1,0) can take it to state (0,1). Thus, in the up–down model, the stable manifold must be curved since strong depolarizing inputs can also cause a switch from up to down. Figure 11.5c shows that the stable manifold of the saddle point curves around, so if a stimulus takes the excitatory population beyond about 0.4, then there will be an immediate return to the down state. Modest stimuli will take the system from the down to the up state and vice versa. Other properties of the up–down states follow immediately. For example, a depolarizing shock in the up state can take the system to the down state. Shu et al. [247] observed that there is a delay before going to the down state which is dependent on the amplitude of the stimulus. As can be seen in the figure, a stimulus which is close to the stable manifold but slightly beyond the right-hand branch will take much longer to go to the down state than will a stronger stimulus. Strong stimuli during the down state can induce a brief period of activation followed by a return to the down state as well. Adding a small amount of noise to the model equations can cause spontaneous transitions between up and down states much as is seen in Fig. 11.5a. Because the upper state is closer to instability and has complex eigenvalues, this could explain the fact that the upper state is much noisier than the lower state. Indeed, Volgushev et al. [280] used the large standard deviation of the "up state" as a means of automatically determining when neurons are in the up state.

11.3.3.2 Whisker Barrels

Everyone who has ever had the pleasure of playing with a rat knows that the rat has several rows of whiskers which it uses to feel the world around it. Indeed, the usual white laboratory rats, which are popular with neuroscientists, are virtually blind and use their whiskers to navigate in their environment. Rats' whiskers are almost as sensitive as human fingers in discriminating textures. Each whisker projects (through the brainstem and then the thalamus) to a well-defined aggregate of neurons in layer 4 of the cortex in the somatosensory area. These discrete areas are called barrels (see Fig. 11.6a, b) and consist of a mixture of excitatory (70%) and inhibitory (30%) neurons which are recurrently connected. Thus, the local circuitry of the barrel is a perfect example of an excitatory–inhibitory network. Inputs to the barrel come from other layers of cortex and from the thalamus. In this example, we restrict our attention to the local recurrent interactions and the thalamic inputs as shown in Fig. 11.6c. Dan Simons [218] and his collaborators have shown that the barrel circuit is exquisitely sensitive to the timing of the inputs from the thalamus. That is, the barrels respond strongly to rapidly increasing inputs and weakly to slow inputs. Figure 11.6d shows a typical example. The left-hand response is very large compared to the right-hand one and the corresponding thalamic inputs show a rapid onset and a more gradual onset. Pinto et al. [217] reduced a large-scale spiking model due to [168] to a network which should be familiar to the reader by now:

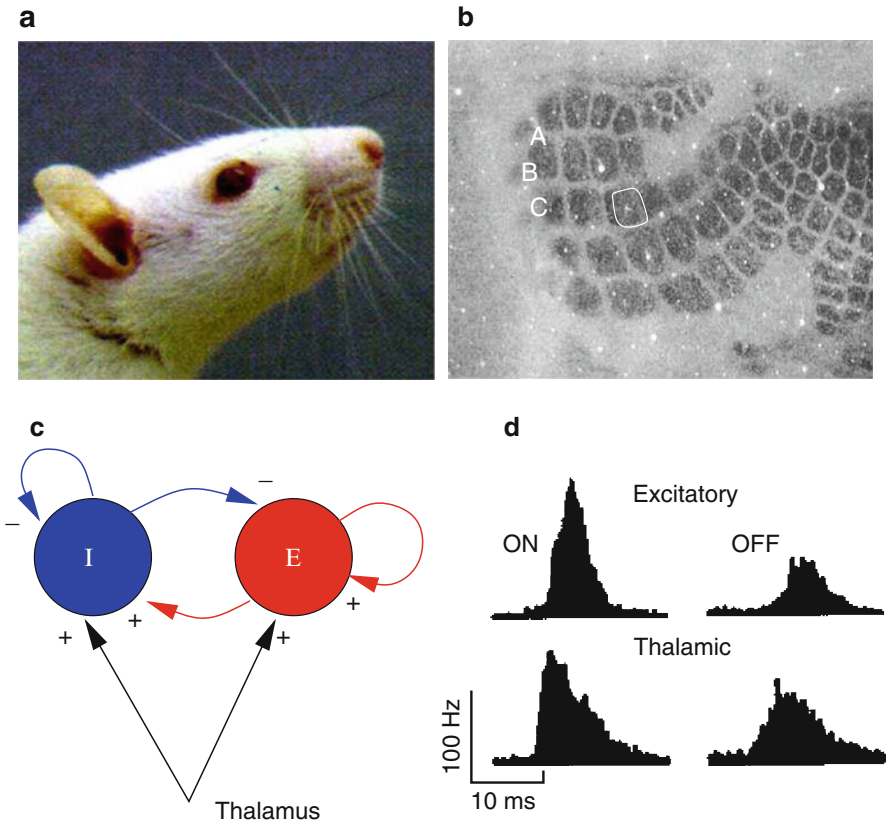

Fig. 11.6 Whisker barrel system of the rat. (**a**) Rat face. (**b**) Layer 4 cortex in the whisker area of the rat showing discrete barrels corresponding to individual whiskers. The C3 barrel is *circled*. (**c**) Local circuitry within a barrel showing a strongly recurrent excitatory and inhibitory network along with thalamic input. (**d**) Population response of excitatory cells to experimental movement of a whisker. Thalamic response is also shown

$$\tau_e \frac{\mathrm{d}u}{\mathrm{d}t} = -u + F_e(w_{ee}u - w_{ie}v + w_{te}T(t)),$$
$$\tau_i \frac{\mathrm{d}v}{\mathrm{d}t} = -v + F_i(w_{ei}u - w_{ii}v + w_{ti}T(t)).$$

The thalamic input, $T(t)$, consists of a constant background activity plus a triangle lasting 15 ms. The height of the triangle is constant, but the onset slope can be varied. The question is whether the network responds differently to different slopes of input. The input drives both the inhibition and the excitation, which is crucial. Intuitively, if the slope is too small, then the inhibition can catch up and suppress the excitation. This provides what experimentalists call a "window of opportunity" for the barrel cells to produce a response.

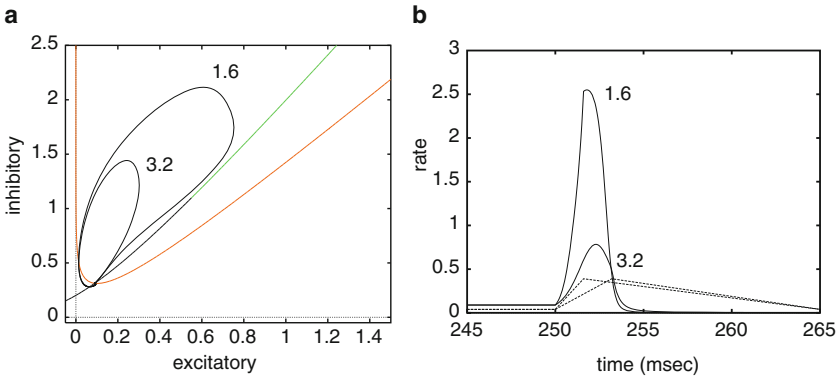

Fig. 11.7 Simulation of the barrel network. (**a**) Phase plane for the barrel network at rest with two responses superimposed corresponding to input peaks at 1.6 and 3.2 ms. (**b**) Firing rate of the excitatory population for the two inputs in (**a**) along with the inputs themselves (*dashed lines*). $F_e(x) = 5.12/(1 + \exp(-(x - 15)/4.16))$, $F_i(x) = 11.61/(1 + \exp(-(x - 15)/3.94)$, $w_{ee} = 42, w_{ie} = 24.6, w_{ei} = 42, w_{ii} = 18, \tau_e = 5, \tau_i = 15, w_{te} = 53.43, w_{ti} = 68.4$

Figure 11.7a shows that in the absence of inputs, the barrel network has a stable resting state. A perturbation in the excitatory direction past the right (middle) branch of the excitatory nullcline will be greatly amplified before returning to rest (an example of an excitable system). However, in the barrels, inputs come into both the excitatory and the inhibitory cells, so it is not clear what type of response occurs. Two responses are shown in the phase plane and in the accompanying plot in Fig. 11.7b corresponding to triangle inputs which have a width of 15 ms and identical amplitude. The only difference is that they reach the peak amplitude at 1.6 and 3.2 ms, respectively. By rising more quickly, the excitatory cells have a chance to react before the inhibition is engaged. The result is a significantly larger response for the fast-rising inputs compared with the slower-rising ones.

11.3.4 Generalizations of Firing Rate Models

Various bells and whistles can be added to firing rate models to match their architecture with a more biologically realistic one. For example, many cortical neurons are endowed with spike-frequency adaptation which occurs on a much slower timescale than inhibition and is dependent only on the local neuron rather than on other neurons. Another example is short-term synaptic plasticity such as the depression or facilitation of synapses. Adaptation can be introduced as an activity-dependent negative feedback. For example, a single excitatory population with adaptation can be written as

$$\begin{aligned} \tau \frac{\mathrm{d}u}{\mathrm{d}t} &= F(au - cz), \\ \tau_z \frac{\mathrm{d}z}{\mathrm{d}t} &= R(u, z) - z, \end{aligned} \tag{11.27}$$

where $R(u, z)$ is the activation of adaptation by excitation. There are several different possible models of this. The simplest is that $R(u, z) = u$. This linear adaptation allows for various interesting dynamics. If we recall that F is actually the firing rate, then a more realistic model would be $R(u, z) = \alpha F$ and if there was saturation (as would be the case if the adaptation were based on the conductance of some channel), then

$$R(u, z) = \alpha F(1 - z).$$

This ensures that the adaptation can never exceed 1. The reader should explore this model on her own choosing, for example, $\tau_z \gg \tau$.

Synaptic depression (or facilitation) is more interesting as its effects are multiplicative. Let us recall the model for short-term depression of a synapse (7.14) from Chap. 8 (8.13):

$$\frac{\mathrm{d}d}{\mathrm{d}t} = \frac{1 - d}{\tau_d} - \left(\sum_j \delta(t - t_j) \right) a_d d,$$

where t_j are the spike times of the presynaptic neuron, a_d is the degree of depression, and τ_d is the rate of recovery back to full strength. If we average this model over many repetitions of the same process, then the spike times are replaced by the firing rate of the presynaptic cell; thus, in terms of the firing rate, the model for synaptic depression is

$$\frac{\mathrm{d}d}{\mathrm{d}t} = \frac{1 - d}{\tau_d} - a_d F d.$$

We remark that several authors replace F in the above equation by u, which is often also called the firing rate. Depending on the interpretation and derivation of the firing rate, either can be correct. If the firing rate models are derived from synaptic dynamics, then F is the firing rate, but if we are approximating a noisy model neuron response to inputs, then u is the approximation of the firing rate.

We illustrate extended firing rate models by looking at two examples.

11.3.4.1 Binocular Rivalry

When a person looks at two different objects in each of his eyes, such as vertical stripes in the left and horizontal in the right, then he does not perceive a mixture, but rather he sees only one or the other. After a second or two the dominant percept disappears and the other object becomes dominant. Then there is another switch and so on. The switching is random, but there is a peak in the switching time histogram. There have been dozens of models for this kind of behavior, starting with that in [178] and recently reviewed and summarized in [246]. As there is a preferred interval for switching, many models assume the switching is governed by some sort of oscillator. We will start with the competitive model, (11.23), but add the additional adaptation

$$\begin{aligned} u_1' &= -u_1 + F(I - wu_2 - gz_1), \\ z_1' &= (u_1 - z_1)/\tau, \\ u_2' &= -u_2 + F(I - wu_1 - gz_2), \\ z_2' &= (u_2 - z_2)/\tau. \end{aligned} \tag{11.28}$$

Here, u_1 represents the right-eye pattern and u_2 represents the left-eye pattern. If the degree of adaptation, g, is small enough, then we expect the behavior should be like that of (11.23); for large enough w, as I increases there will be a pitchfork bifurcation from the homogeneous state to a state when one or the other "wins." Because of symmetry, either left or right can win. As in the competitive model, there will be a homogeneous resting state, $(u_1, z_1, u_2, z_2) = (\bar{u}, \bar{u}, \bar{u}, \bar{u})$. The stability of this state is found by studying the eigenvalues of a 4×4 matrix:

$$M = \begin{pmatrix} -1 & -cg & -cw & 0 \\ 1/\tau & -1/\tau & 0 & 0 \\ -cw & 0 & -1 & -cg \\ 0 & 0 & 1/\tau & -1/\tau \end{pmatrix} = \begin{pmatrix} A & B \\ B & A \end{pmatrix},$$

where A and B are 2×2 matrices and $c = F'(I - (w+g)\bar{u})$. Just like the competition model, the structure of M has symmetry, so we can reduce the computation of the eigenvalues to those of two 2×2 matrices, $C^+ = A + B$ and $C^- = A - B$. These two matrices correspond to eigenvectors of the form (x, y, x, y) and $(x, y, -x, -y)$. The former represents symmetric perturbations of the steady state and the latter represents asymmetric ones. Consider, first, symmetric perturbations:

$$C^+ = \begin{pmatrix} -1 - cw & -cg \\ 1/\tau & -1/\tau \end{pmatrix}.$$

Since C^+ has a negative trace (recall that $F' > 0$, so c is positive and w and g are nonnegative) and a positive determinant, all eigenvalues of C^+ have negative real parts. The asymmetric perturbations are more interesting:

$$C^- = \begin{pmatrix} -1 + cw & -cg \\ 1/\tau & -1/\tau \end{pmatrix}.$$

If we treat c as a parameter (this is related to the intensity of the stimulus and, of course, the shape of F), then the determinant vanishes when $w > g$ and $c = c_0 \equiv 1/(w - g)$ and the trace vanishes when $c = c_H \equiv 1/w(1 + 1/\tau)$. Thus, if g is close to w and τ is large, the trace will become positive at smaller inputs than it takes to make the determinant negative. That is, there will be a Hopf bifurcation as the input increases when the time constant of adaptation is large and the strength of adaptation is also sufficiently large. In contrast, with weak or very fast adaptation, the network

will maintain its winner-take-all behavior. This simple mechanism provides a means by which there will be periodic switching of the dominance of the two percepts. Although this is a somewhat naive model, it is able to explain some aspects of rivalry and, in fact, make some testable predictions [289]. We will leave the full numerical exploration of this model as an exercise for the reader.

11.3.4.2 Synaptic Depression and Oscillations

Many neuronal networks show spontaneous oscillations during development; it is believed that the activity may help strengthen connections between neurons which are important later in the animals life. A striking example of this is spontaneous episodes of activity in the spinal cord of embryonic chickens. Isolated spinal cord preparations produce bursts of activity every 2–30 min and within these bouts of activity produce 0.1–2-Hz oscillations. Tabak et al. [257] suggested the mechanism underlying this is recurrent excitatory connections coupled to synaptic depression with two different timescales. The slow depression accounts for the long interburst interval and the faster depression accounts for the oscillations within a burst. Here, we will be concerned only with the higher-frequency oscillations. Let $u(t)$ denote the firing rate of the population and $d(t)$ the efficacy of the synapse. Then the equations are

$$\begin{aligned} u' &= -u + f(wdu), \\ \tau d' &= 1 - d - \alpha u d. \end{aligned} \tag{11.29}$$

Our model for d is slightly different from the one in Tabak et al., but the nullclines are qualitatively similar. In the Tabak et al. paper, they used

$$f(x) = 1/(1 + \exp(-(x - \theta)/k)),$$

with $k = 0.05$ and $\theta = 0.18$. By choosing $w = 1, \alpha = 5$, and $\tau = 5$, we can obtain sustained oscillations. We leave a complete analysis of this to the reader. A related model and phenomenon is found in [273].

11.3.5 Beyond Mean Field

The Wilson–Cowan equations (11.18) and their kin are meant to represent the mean-field dynamics of networks of many thousands of individual neurons. Often, there is a desire to understand how higher-order statistical fluctuations influence the dynamics. For example in the work reported in [32], some of the dynamics arises from fluctuations rather than from the mean field. A number of authors, notably Buice and Cowan [29] and Bressloff [21], have attempted to include fluctuations

in the mean-field models by creating a stochastic system which has the desired mean-field dynamics. From this model stochastic system, they derived an expansion to include higher-order statistics such as the correlations between populations. As with any noisy nonlinear system, the difficulty arises when computing the moments (mean, variance, etc.) since, for example, the mean depends on second-order, third-order, etc. statistics. We saw in Chap. 10 that approximations could be made in the weak-noise limit for stochastic differential equations. We also saw that it is possible to approximate a Markov channel model by a simple Langevin equation via (10.38) and (10.39). We can combine these two approaches to arrive at a very simple derivation of the system size expansion given in [21]. For simplicity, we will consider just one population of neurons and leave the case of two populations and beyond as an exercise. Let there be N neurons whose state, x_i, can be either be silent (0) or active (1). Each neuron is coupled to all the other neurons in an identical fashion with weight w/N. The transition from active to silent occurs at a constant rate, α, and the transition from silent to active occurs at rate

$$\beta := f\left(\frac{1}{N}\sum_{i=1}^{N} x_i\right).$$

Thus, we can think of these "neurons" as two-state "channels." The mean field for the firing neurons (open channels) is

$$\frac{\mathrm{d}m}{\mathrm{d}t} = -\alpha m + f(m).$$

This equation is like any other mean-field model that we have already considered in this chapter. To get higher-order statistics, we use the Langevin approximation from Chap. 10 [(10.38) and (10.39)]:

$$\frac{\mathrm{d}m}{\mathrm{d}t} = -\alpha m + f(m) + \left(\frac{\alpha + f(m)}{N}\right)^{\frac{1}{2}} \mathrm{d}W(t). \tag{11.30}$$

We assume N is large and apply the Rodriguez–Tuckwell small-noise expansion to this Langevin equation and arrive at the pair of equations

$$\frac{\mathrm{d}m}{\mathrm{d}t} = -\alpha m + f(wm) + \frac{1}{2}w^2 f''(wm)C, \tag{11.31}$$

$$\frac{\mathrm{d}c}{\mathrm{d}t} = -2\alpha C + 2w f'(wm)C + \frac{1}{N}[\alpha m + f(wm)]. \tag{11.32}$$

This is equivalent to the system-size expansion in [21].

11.4 Some Methods for Delay Equations

Delay equations do not commonly appear in the curricula of most dynamics courses so we review a number of well-known results mostly from the classic text of Bellman and Cooke [13]. Here, we focus on systems with only one delay and only consider the linear stability theory around equilibria for delay equations. We start with a simple scalar example,

$$\frac{\mathrm{d}x}{\mathrm{d}t} = f(x(t), x(t-\tau)),$$

and let $\bar{x}$ be a fixed point, $f(\bar{x}, \bar{x}) = 0$. The linearized equation has the form

$$\frac{\mathrm{d}y}{\mathrm{d}t} = ay(t) + by(t-\tau).$$

Here, a and b are the derivatives of f with respect to the first and second arguments evaluated at the fixed point. As with ordinary differential equations, we look for solutions of the form $y(t) = \exp(\lambda t)$, leading to

$$\lambda = a + b\mathrm{e}^{-\lambda\tau}.$$

There are infinitely many roots of this equation; if any of them has a positive real part, then we say the fixed point is unstable. If all roots have negative real parts, then the fixed point is linearly asymptotically stable. For general systems with one delay, if the delay appears only in one variable, then the characteristic equation will take the form

$$M(\lambda) \equiv P(\lambda) + Q(\lambda)\mathrm{e}^{-\lambda\tau} = 0.$$

Thus, for many commonly encountered problems, the stability of fixed points relies on solving the polynomial–exponential characteristic equation. Before stating some theorems about stability, we consider a more general question: can a delay destabilize a fixed point which, in the absence of delay, was stable? Stability can be lost via a zero eigenvalue or through complex conjugate eigenvalues. In the former case, one must have $P(0) + Q(0) = 0$, which is clearly independent of the delay. Thus, we focus on determining if it is possible for a delay to cause $M(\lambda)$ to have imaginary eigenvalues. If this happens, then

$$\Gamma(\omega) \equiv \frac{P(\mathrm{i}\omega)}{Q(\mathrm{i}\omega)} = \mathrm{e}^{-\mathrm{i}\omega\tau}.$$

The left-hand side of this expression traces out a curve in the complex plane (see Fig. 11.8) and the right-hand side traces out the unit circle. Suppose $\Gamma(0)$ lies outside the unit circle and as ω varies it never crosses the circle (case 1). Then, there will be no delay τ which can change the stability, since the two curves never intersect. If $\Gamma(0)$ is inside the unit circle and never leaves it, then, again, no stability change can

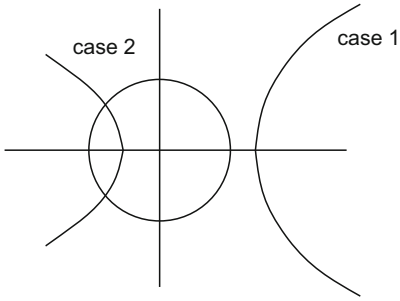

Fig. 11.8 Stability plots for delay equations

occur. However, if $\Gamma(\omega)$ and the unit circle intersect (case 2), then we can always choose τ so that they intersect at the same value of ω. Thus, we can destabilize the equilibrium by changing the delay. Since the critical eigenvalue is $i\omega$, we expect to get a bifurcation to periodic orbits, although the proof of this is much more difficult than that of the ordinary differential equation case. As an example, consider the above scalar problem.

$$\Gamma(\omega) = \frac{i\omega - a}{b}.$$

This traces a vertical line in the complex plane. If $|a/b| < 1$, then $\Gamma(\omega)$ will cross the unit circle and there will be delay-induced instability. Note that for the fixed point to be stable in the absence of a delay, we have $a + b < 0$. For delay-induced instability, the magnitude of b must be larger than a, so these two inequalities imply that b is negative and sufficiently large. We have thus shown a classic result that delayed negative feedback can induce oscillations.

We conclude with a theorem from Bellman and Cooke giving general results for scalar delay equations. We rewrite the characteristic equation as

$$e^{\lambda\tau} P(\lambda) + Q(\lambda) = 0$$

and let $z = \lambda\tau$. Since $\tau > 0$, if z has a positive real part, then so does λ. The following theorem provides necessary and sufficient conditions for stability of the scalar delay equations, which can be written as $H(z) = \tau a e^z + b\tau - z e^z = 0$.

Theorem. (Bellman and Cooke [13], p. 444). *All roots of* $pe^z + q - ze^z$ *have negative real parts if and only if*

(*a*) $p < 1$ *and*
(*b*) $p < -q < \sqrt{r_1^2 + p^2}$,

where r_1 *is a root of* $r = p \tan r$ *such that* $0 < r < \pi$. *If* $p = 0$, *we take* $r_1 = \pi/2$.

Using this theorem as well as the easy graphical method above, you should have no trouble solving the problems for delay equations.

11.5 Exercises

1. Derive (11.3).
2. We can write (11.3) as

$$\Phi(t) = Ae^{-at} + Be^{-bt} + Ce^{-ct},$$

where a, b, and c are positive numbers. Show that A, B, and C are such that $\Phi(0) = \Phi'(0) = 0$. (Note the first part is by definition. Use the definition of $\Phi(t)$ to prove the second part.) Now that you have done that, suppose

$$x(t) = \int_0^t \Phi(t-s)y(s)\mathrm{d}s.$$

What third-order differential equation does $x(t)$ satisfy?
3. Consider the scalar neural network

$$u'' + (a+b)u' + abu = F(u),$$

where a and b are positive. Prove there can be no limit cycle solutions. Suppose $F(0) = 0$. What types of bifurcations are possible?
4. In Exercise 2 you showed that the general $\Phi(t)$ leads to a third-order differential equation. Consider the scalar neural network

$$[(\mathrm{d}/\mathrm{d}t + a)(\mathrm{d}/\mathrm{d}t + b)(\mathrm{d}/\mathrm{d}t + c)]u = F(\alpha u).$$

Suppose $F' > 0$ and a, b, and c are positive. For $\alpha < 0$ show that there exists a unique fixed point and show that a Hopf bifurcation is possible as one of the parameters varies. (Hint: Think about the Routh–Hurwitz criteria.) If $\alpha > 0$, show there cannot be a Hopf bifurcation. We conjecture that there can be no periodic solutions if $\alpha > 0$, but have no proof.
5. Derive (11.14).
6. Consider the delayed excitatory network

$$u_t + u = F(\alpha u(t-\tau)),$$

where we have set $\tau_m = 1$ without loss of generality. Assume $F'(u) > 0$ and $\alpha > 0$. Prove there exists at least one fixed point and prove there can never be a Hopf bifurcation no matter what the delay.
7. Consider the delayed inhibitory network

$$u_t + u = F(-\alpha u(t-\tau)),$$

where $F(u) \geq 0$, $F'(u) > 0$, and $\alpha > 0$. Prove there is a unique fixed point (see the next exercise) and that there can be a Hopf bifurcation. Simulate this

network using $F(u) = 1/(1 + \exp(-(u + I))$, where I is input to the network. Use $\alpha = 8$ and $I = 1$ and treat τ as a parameter.

8. Suppose $G(u) \geq 0$ and $G'(u) < 0$ for all u. Prove there is a unique root fixed point of

$$u_t + u = G(u)$$

and that it is asymptotically stable.

9. Consider (11.12). (a) If $F(I) = \sqrt{I - I^*}$ for $I > I^*$ and is zero otherwise, compute $F_Q(I)$ when $I*$ is taken from a uniform distribution $I_{\min} \leq I^* \leq I_{\max}$. (b) If $F(I - I^*) = \max(I - I^*, 0)$ and I^* is taken from a Gaussian distribution with mean $\bar{I}$ and standard deviation σ, compute $F_Q(I)$. (c) Repeat (b) for $F(I - I^*) = 1$ for $I > I^*$ and zero otherwise.

10. Compute the firing rate function for the integrate-and-fire model based on the conductance of the synapse. That is, suppose V satisfies

$$C\frac{\mathrm{d}V}{\mathrm{d}t} = -g_{\mathrm{L}}(V - E_{\mathrm{L}}) - g(V - E_{\mathrm{syn}}),$$

where $E_{\mathrm{L}} < V_{\mathrm{T}} < E_{\mathrm{syn}}$ is the threshold to spiking and that upon spiking V is reset to $E_{\mathrm{r}} < V_{\mathrm{T}}$. Compute the firing rate as a function of the synaptic conductance, g. What happens as $g \to \infty$? Can you do some asymptotics of this to get a simple formula for large conductances? Plot the F–g curve for $C = 1$, $g_{\mathrm{L}} = 0.05$, $E_{\mathrm{L}} = -65$, $E_{\mathrm{r}} = -70$, $E_T = -50$, and $E_{\mathrm{syn}} = 0$.

11. Consider a recurrent scalar network with the threshold linear firing rate

$$\frac{\mathrm{d}u}{\mathrm{d}t} = -u + [au - u_T]_+.$$

Show if $a > 1$, then sufficiently large initial conditions grow exponentially. For a fixed positive value of u_T and $a > 1$, find the critical value of u_0 such that if $u(0) > u_0$, $u(t)$ grows exponentially without bound.

12. Suppose $F(u) \geq 0$, $F'(u) > 0$, and $F''(u)$ has a single zero. Assume F and its derivatives are continuous on R. Prove there are at most three fixed points of the neural network equation $u' = -u + F(u)$.

13. *Hard*. Suppose $F'(u) \geq 0$ and $F(u)$ has k inflection points. Show that there can be up to $k + 2$ fixed points of $u = F(u)$. (Hint: Use the previous exercise and proceed inductively.)

14. Find the saddle–nodes and the cusp bifurcation for the scalar model with $F(u) = 1/(1 + \exp(-u))$. (Note that $F' = F(1 - F)$.)

15. Prove if $f_y g_x > 0$ in the plane, there are no limit cycles to $x' = f(x, y)$, $y' = g(x, y)$. Here, is a brief hint to get you started. For there to be a limit cycle, $x'(t)$ must change sign. Suppose, first, $f_y > 0$ and $g_x > 0$. (The other case follows similarly.) Suppose $x'(t)$ is positive and then vanishes at $t = t_1$. We cannot have $y'(t_1) = 0$ since then we would be at a fixed point. Thus, either $y'(t_1) > 0$ or $y'(t_1) < 0$. Suppose we have the first case. Then, $x''(t_1) =$

$f_y y'(t_1) > 0$, so for $t > t_1$ $x'(t) > 0$, so x' does not change sign. Continue to argue in this manner for all the other cases. You will need to use the fact that $g_y > 0$ for this.

16. Prove if $F'(u) > 0$, $F(u) > 0$, and $F(-\infty) = 0$, then there is a unique solution to
$$u = F(I - wu)$$
for all I and $w > 0$. Prove u is a monotonically increasing function of I and that $u > 0$. Prove u is a monotonically decreasing function of w.
17. In the mutual interaction model (11.23), what happens if the interaction is positive (that is, $-w$ is positive)? Show that asymmetric perturbations are always stable.
18. *Disinhibition and epilepsy*. One model for epilepsy is that it arises when the inhibition is partially blocked. Consider the Wilson–Cowan model:
$$\begin{aligned} u_1' &= -u_1 + F(12u_1 - 12u_2 - 3), \\ 3u_2' &= -u_3 + F(18u_1 - 4u_2 - 5). \end{aligned}$$
Show through simulation that there is a unique stable equilibrium. Now, suppose a drug such as bicuculline is applied which has the effect of reducing the inhibitory strength. Incorporate a parameter p in the model multiplying the strength of inhibition (do not forget the inhibitory–inhibitory connection) such that when $p = 1$ the inhibition is at full strength and when $p = 0$ it is completely blocked. Compute the bifurcation diagram for the model as p decreases and show that there can be a Hopf bifurcation and for severely reduced inhibition a completely active state.
19. Consider the binocular rivalry model described by (11.28) with $w = 5$, $g = 1, \tau = 20$, and $F(x) = 1/(1 + \exp(-(x - 2)))$. Compute the bifurcation diagram of this model as a function of the parameter I. Now set $g = 0.25$ and compute the diagram again. Note that there is no Hopf bifurcation and there is only the pitchfork. Set $g = 0.5$ and compute as much as you can of the bifurcation diagram. Find the curve of branch points and Hopf points as a function of the two parameters g and I.
20. Use the ideas of (11.30) to derive the five-dimensional equivalents of the Wilson–Cowan equations with means and second-order statistics.

11.6 Projects

1. Consider a pair of neurons (excitatory and inhibitory) coupled as
$$\begin{aligned} u_e(t) &= F_e(w_{ee}\Phi_{ee} * u_e(t) - w_{ei}\Phi_{ei}(t) * u_i(t)), \\ u_i(t) &= F_i(w_{ie}\Phi_{ie} * u_e(t) - w_{ii}\Phi_{ii}(t) * u_i(t)), \end{aligned}$$

where $\Phi_{jk}(t) = \exp(-t/\tau_{ij})/\tau_{ij}$ and $U(t) * V(t) = \int_0^t U(t-s)V(s)\mathrm{d}s$. If τ_{ij} is independent of i or independent of j, then these can be converted to a pair of first-order differential equations. However, if all τ_{ij} are different, then these integral equations can be converted into four first-order differential equations. Write down these four equations. Is there any behavior (e.g., limit cycles) that occurs for the four-equation model which would not occur for the two-equation model when τ_{ij} is independent of i or j? For example, can you prove a fixed point for the four-variable model is asymptotically stable if it is stable for the two-variable model?

2. Consider a noisy integrate-and-fire model, $V' = -V + I$, for which the current makes a step from I_1 to I_2. Using the Fokker–Planck equation, examine the temporal dynamics on the firing rate for this transition in the low- and high-noise regimes ($\sigma = 0.4, 1$). In the low-noise case, the approach to the steady-state rate f is a damped oscillation. For different steps in the current, estimate both the damping and the oscillation rate. The figure below illustrates an example of a step and a fit to a damped oscillation. Use this to suggest a linear model for the firing rate:

$$u'' + 2au' + (a^2 + f^2)(u - f) = 0,$$

where f is the instantaneous firing rate. It may be necessary to also include the derivative of f in the calculation. You will find that for slowly varying stimuli, this does not do any better than the simple ad hoc first-order equation, $\tau_f u' = f - u$.

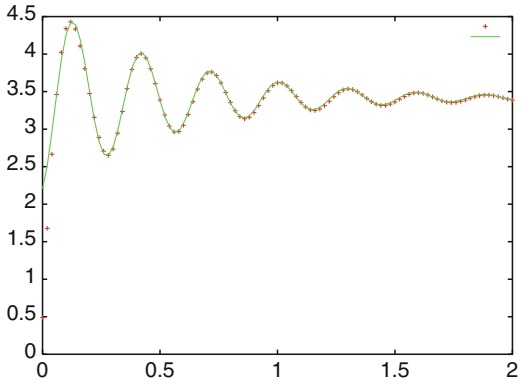

3. On the basis of the previous exercise, the temporal dynamics of the response of a neuron depends on the steady-state firing rate. Consider the same equation as in the previous exercise, but f now depends on u as

$$f = F(wu - u_{\mathrm{th}}),$$

where F is a nonlinear function as explored in this chapter. Do the dynamics of the scalar recurrent network exhibit anything new? Show that even this second-order model cannot produce limit cycle oscillations.

4. Explore the effects of changing the temporal dynamics of inhibition on the barrel network. For example, quantify how that "window of opportunity" depends on the time constant of the inhibitory response.
5. Volgushev et al. [280] looked at the propagation of down to up and up to down transitions in cortex by recording over a 12-mm spatial area in the cat cortex during sleep. Adapt the population model for up–down states to an array of, say, nearest -neighbor coupled populations and add independent noise to each population sufficient to induce spontaneous switching. Do you see any evidence for propagation of states, e.g., if one group of cells switches from down to up, does this switch propagate across the network? Explore different levels of noise and different degrees of coupling. To couple two networks, you should look at a model of the form

$$\tau_e u_j' + u_j = F_e(w_{ee}\bar{u}_j - w_{ie}\bar{v}_j),$$

where

$$\bar{u}_j = (1-c)u_j + (c/2)[u_{j+1} + u_{j-1}]$$

and $c \geq 0$ is the degree of coupling. Similar equations for the inhibitory population, v_j, should be written as well with a possibly different coupling strength. Use parameters as in Fig. 11.5.